ANTIOXIDANTS & REDOX SIGNALING
Volume 23, Number 9, 2015

DOI: 10.1089/ars.2015.6265

Discoveries

ORIGINAL RESEARCH COMMUNICATION

# When an Intramolecular Disulfide Bridge Governs the Interaction of DUOX2 with Its Partner DUOXA2

Aurore Carré,[1–3,*] Ruy A.N. Louzada,[1,4,*] Rodrigo S. Fortunato,[4] Rabii Ameziane-El-Hassani,[1–3] Stanislas Morand,[5,†] Vasily Ogryzko,[6] Denise Pires de Carvalho,[4] Helmut Grasberger,[7] Thomas L. Leto,[5] and Corinne Dupuy[1–3]

## Abstract

***Aims:*** The dual oxidase 2 (DUOX2) protein belongs to the NADPH oxidase (NOX) family. As $H_2O_2$ generator, it plays a key role in both thyroid hormone biosynthesis and innate immunity. DUOX2 forms with its maturation factor, DUOX activator 2 (DUOXA2), a stable complex at the cell surface that is crucial for the $H_2O_2$-generating activity, but the nature of their interaction is unknown. The contribution of some cysteine residues located in the N-terminal ectodomain of DUOX2 in a surface protein–protein interaction is suggested. We have investigated the involvement of different cysteine residues in the formation of covalent bonds that could be of critical importance for the function of the complex. ***Results:*** We report the identification and the characterization of an intramolecular disulfide bond between cys-124 of the N-terminal ectodomain and cys-1162 of an extracellular loop of DUOX2, which has important functional implications in both export and activity of DUOX2. This intramolecular bridge provides structural support for the formation of interdisulfide bridges between the N-terminal domain of DUOX2 and the two extracellular loops of its partner, DUOXA2. ***Innovation:*** Both stability and function of the maturation factor, DUOXA2, are dependent on the oxidative folding of DUOX2, indicating that DUOX2 displays a chaperone-like function with respect to its partner. ***Conclusions:*** The oxidative folding of DUOX2 that takes place in the endoplasmic reticulum (ER) appears to be a key event in the trafficking of the DUOX2/DUOXA2 complex as it promotes an appropriate conformation of the N-terminal region, which is propitious to subsequent covalent interactions with the maturation factor, DUOXA2. *Antioxid. Redox Signal.* 23, 724–733.

## Introduction

THE DUAL OXIDASE 2 (DUOX2) protein belongs to the NADPH oxidase (NOX/DUOX) family. DUOX2 and its counterpart, DUOX1, were initially identified as $H_2O_2$ sources involved in thyroperoxidase-mediated iodide organification during thyroid hormone biosynthesis (4, 5). The discovery of congenital hypothyroidism resulting from in-

### Innovation

Both stability and function of the maturation factor, dual oxidase activator 2 (DUOXA2), are totally dependent on the oxidative folding of dual oxidase 2 (DUOX2), indicating that DUOX2 displays a chaperone-like function with respect to its partner.

[1]Université Paris-Sud, Orsay, France.
[2]UMR 8200 CNRS, Villejuif, France.
[3]Institut Gustave Roussy, Villejuif, France.
[4]Laboratório de Fisiologia Endócrina Doris Rosenthal, Instituto de Biofísica Carlos Chagas Filho, Universidade Federal do Rio de Janeiro, Rio de Janeiro, Brazil.
[5]Laboratory of Host Defenses, National Institute of Allergy and Infectious Diseases, National Institutes of Health, Rockville, Maryland.
[6]UMR 8126 CNRS, Villejuif, France.
[7]Department of Internal Medicine, Division of Gastroenterology, University of Michigan, Ann Arbor, Michigan.
*These authors contributed equally and should be considered joint first authors.
[†]*Current affiliation:* L'OREAL Advanced Research, Aulnay-sous-bois, France.

activating mutations of the *DUOX2* gene highlighted that DUOX2 is actually the main $H_2O_2$ provider of the thyroperoxidase (16–18). Far from being ubiquitous, DUOX2 is not restricted to the thyroid. It is also well expressed in the respiratory tract epithelium and in the gastrointestinal mucosa where it plays a key role in antimicrobial defense (8). Overexpression of the *DUOX2* gene has been associated with an increasing number of inflammation diseases, such as Crohn's disease (2), irritable bowel syndrome (1), and helicobacter-associated gastritis (11).

DUOX2 requires a maturation factor, DUOX activator 2 (DUOXA2), to exit from the endoplasmic reticulum (ER) and reach the apical plasma membrane (9). DUOX2 and DUOXA2 proteins form a stable complex at the cell surface that is fundamental for the enzymatic activity (15).

The heterodimerization of DUOX2 and DUOXA2 is a prerequisite for reactive oxygen species production, but the nature of their interaction is not known (12). The N-terminal peroxidase-like ectodomain of the DUOX proteins differentiates them from other NOX proteins. In previous studies, we showed that mutations of cysteine residues in the N-terminal domain of the human DUOX2 protein affect both targeting and extracellular $H_2O_2$ production by human DUOX2, indicating that these residues are critical for proper maturation of the flavoprotein (7, 14). Disulfide (S-S) bonds, which are promoted and maintained by the oxidizing environment of the ER, play an important role in protein folding, stability, function, and protein–protein interaction (6). Incidentally, unpaired cysteine thiols have been shown to cause ER retention.

In this study, we report the characterization of an intramolecular disulfide bond between the N-terminal domain and the second predicted extracellular loop of DUOX2, which has an important structural implication in both export and activity of DUOX2 by promoting covalent interaction between DUOX2 and its partner, DUOXA2. In addition, this interaction is critical for DUOXA2 stability. Therefore, this study contributes to a change of paradigm regarding the nature of the relationship between the two proteins: DUOX2 displays a chaperone-like function with respect to its functional partner.

## Results

### *Covalent binding between DUOX2 and DUOXA2*

The function of the long extracellular N-terminal domain of DUOX2 remains unclear. Among the possible roles of this domain, it has been proposed that it could play a key role in the interaction with its maturation factor, DUOXA2. The N-terminal region of DUOX2 contains five cysteines (Fig. 1A). These residues might be involved in intra- and intermolecular disulfide bonds that affect the global conformation of the protein. To analyze the role of these cysteine residues in the interaction with DUOXA2, we used the DUOX2 mutants previously constructed where cysteines, 124, 351, 370, 568, or 582, were, respectively, replaced by glycine (7). In addition to that previously observed with whole cells, $H_2O_2$ generation of particulate fractions from mutants C124G, C568G, and C582G DUOX2-transfected cells was completely abolished, whereas the activities of mutants C351G and C370G were only partially decreased (Fig. 1B). This indicated that mutations of cysteine residues affecting membrane translocation abolished both extra- and intracellular activities.

The apparent molecular mass of DUOX2 protein after sodium dodecyl sulfate–polyacrylamide gel electrophoresis (SDS-PAGE) varies depending on the redox environment (10). In reducing conditions, the wild-type (WT) DUOX2 protein coexpressed with DUOXA2 was detected as two bands very close in size, around 185 kDa (3). In nonreducing conditions, the mobility of the WT DUOX2 decreased, and DUOX2 was detected at around 250 kDa. This shift in the electrophoretic mobility from 185 to 250 kDa, which corresponds to the oxidized form of DUOX2 previously described (10), could be explained by the presence of an intramolecular disulfide bond. When such a bond is present, the protein may not fully denature, altering its mobility. This mobility shift is incompatible with DUOX2 dimerization. Importantly, as shown in Figure 1B, only mutation of cysteine 124 totally suppressed the mobility shift of DUOX2, indicating that among the cysteine residues present in the ectodomain, only this cysteine was implied in disulfide bond formation. This bond is not artifactually generated during or after homogenization since all experiments were performed in the presence of 20 m*M* N-ethylmaleimide (NEM) that prevents any aberrant disulfide bond formation. Immunoblot analysis also revealed that mutation of cysteines, 124, 568, and 582, which suppressed DUOX2 activity, significantly affected the level of expression of the maturation factor, DUOXA2. This finding underlined that a correct structural conformation of DUOX2 is essential for the stability of DUOXA2. This was confirmed by using an HEK293 cell line stably expressing DUOXA2 where transfection of WT DUOX2 compared with the mutant DUOX2 C124G highly enhanced the level of expression of DUOXA2 in these cells (Fig. 1C). Therefore, these results show that DUOXA2 functions at a late stage of maturation occurring after oxidative folding of DUOX2.

To investigate whether the DUOXA2 protein is degraded *via* the proteasome-dependent pathway, we examined the expression of DUOXA2 in HEK-293 cells coexpressing mutant DUOX2 C124G after treatment with a proteasome inhibitor, MG132 (Fig. 1D). Treatment of cells with MG132 remarkably enhanced the expression of DUOXA2 in a dose-dependent manner. This had no effect on the $H_2O_2$-generating activity, indicating that the absence of activity in these conditions was mainly due to a misfolding of the DUOX2 N-terminal region itself rather than to a decrease of DUOXA2 expression (Fig. 1E). The same results were obtained with mutant cysteine 582 (Supplementary Fig. S1A; Supplementary Data are available online at www.liebertpub.com/ars). We next assessed the targeting of both DUOXA2 and mutant DUOX2 C124G protein to the plasma membrane in the presence or in the absence of MG132 by flow cytometry and immunofluorescence microcopy. N-terminal myc epitope-tagged DUOXA2 was coexpressed in HEK293 cells with either N-terminal hemagglutinin (HA) epitope-tagged DUOX2 or HA-tagged DUOX2 C124G (Fig. 2A). While WT DUOX2 was well expressed at the cell plasma membrane, no surface signal was obtained for the mutant. This was associated with a total absence of the maturation factor, DUOXA2, at the cell surface. Analysis of cells by confocal microscopy confirmed the retention of DUOXA2 at the ER level when it was coexpressed with the mutant DUOX2 (Fig. 2B). Thus, these findings highlighted that the oxidized form of DUOX2 is essential for both stability and trafficking of DUOXA2 to the cell surface. Immunochemistry analysis of

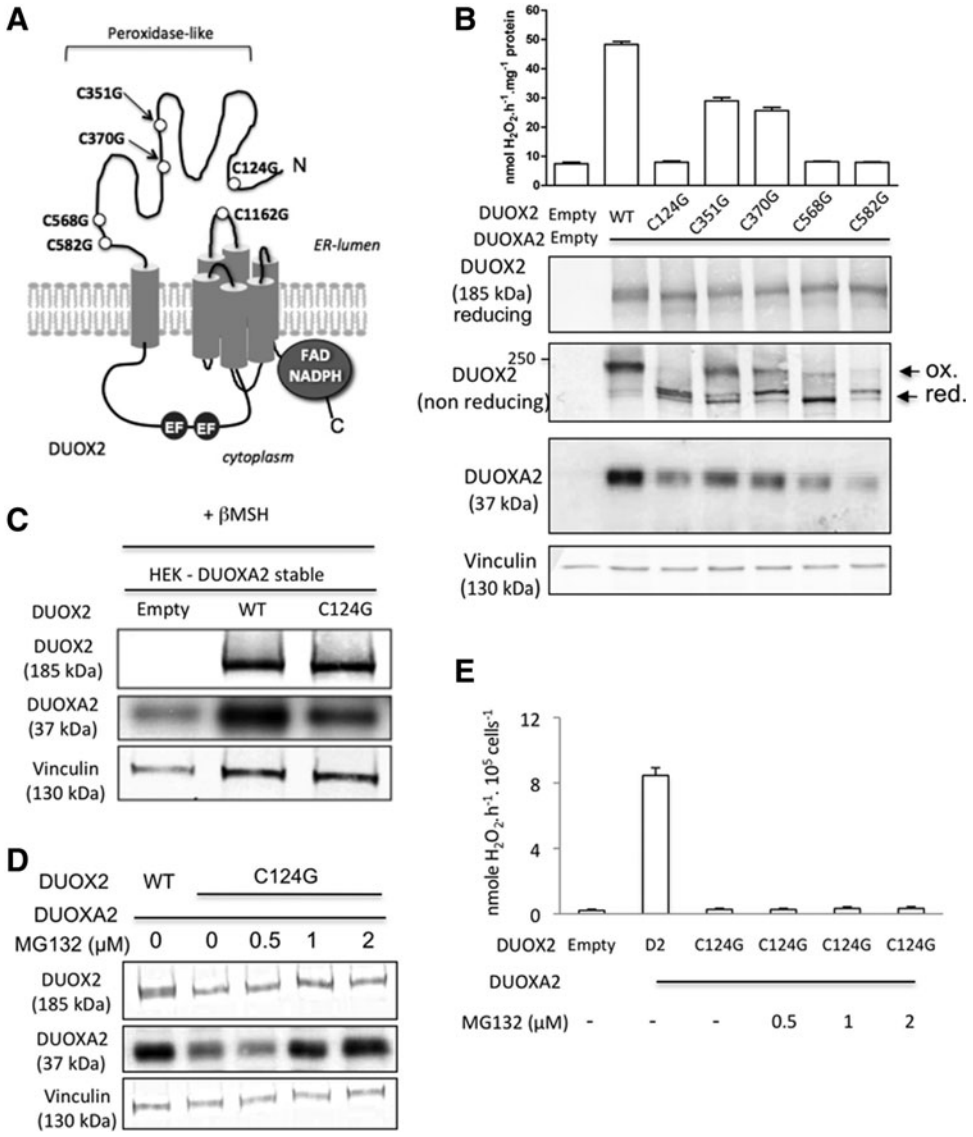


**FIG. 1. Effects of cysteine mutations of ectodomain of DUOX2 on $H_2O_2$ production and on stability of both DUOX2 and DUOXA2 proteins.** **(A)** Schematic representation of DUOX2 with the proposed topology in the membrane. The *circles* indicate the relative positions of mutated cysteine residues. **(B)** NADPH-dependent $H_2O_2$ formation activity in the particulate fraction from HEK-293 cells transiently cotransfected with human DUOX2 or human DUOX2 mutant with human DUOXA2 and from control HEK293 cells (*pcDNA3*). Particulate fractions were incubated as described under the Materials and Methods section. The error bars show the SE of three independent experiments. The Western blot compares the electrophoretic properties of DUOX2 wild-type (WT) and mutant construct proteins under reducing and nonreducing conditions. The reduced and oxidized forms are indicated by *arrows*. The expression of DUOXA2 was analyzed in the same samples. **(C)** Cells stably transfected with human DUOXA2 were transiently transfected with DUOX2 WT or mutant DUOX2 C124G. Proteins were analyzed by Western blot. **(D)** Cells stably transfected with human DUOXA2 were transiently transfected with mutant DUOX2 C124G and treated with vehicle (DMSO) or with different concentrations of MG132 for 12 h. After treatment, DUOX2 and DUOXA2 proteins were analyzed by Western blot. DUOX2 WT was taken as the control. The level of vinculin protein was used as an internal control. **(E)** MG132 treatment does not restore the $H_2O_2$-generating activity of human DUOXA2-HEK293 cells transiently transfected with mutant DUOX2 C124G. DUOX2, dual oxidase 2; DUOXA2, DUOX activator 2.

normal human thyroid tissue confirmed that DUOX2 and its maturation factor, DUOXA2, are both expressed at the apical surface of the thyrocytes (Fig. 2C). The shift of DUOX2 in nonreducing conditions was also observed by immunoblot analysis of total lysate prepared from human thyrocytes.

How the interaction between DUOX2 and DUOXA2 affects the stability of DUOXA2 is unknown. A recent study performed on the purified N-terminal peroxidase-like ectodomain of the counterpart DUOX1 supports the existence of cysteine-mediated disulfide bridges for intermolecular protein–protein interactions (13). Indeed, it is conceivable that an intermolecular disulfide bond between the two proteins may promote the stabilization. To verify this hypothesis, coimmunoprecipitation experiments were carried out.

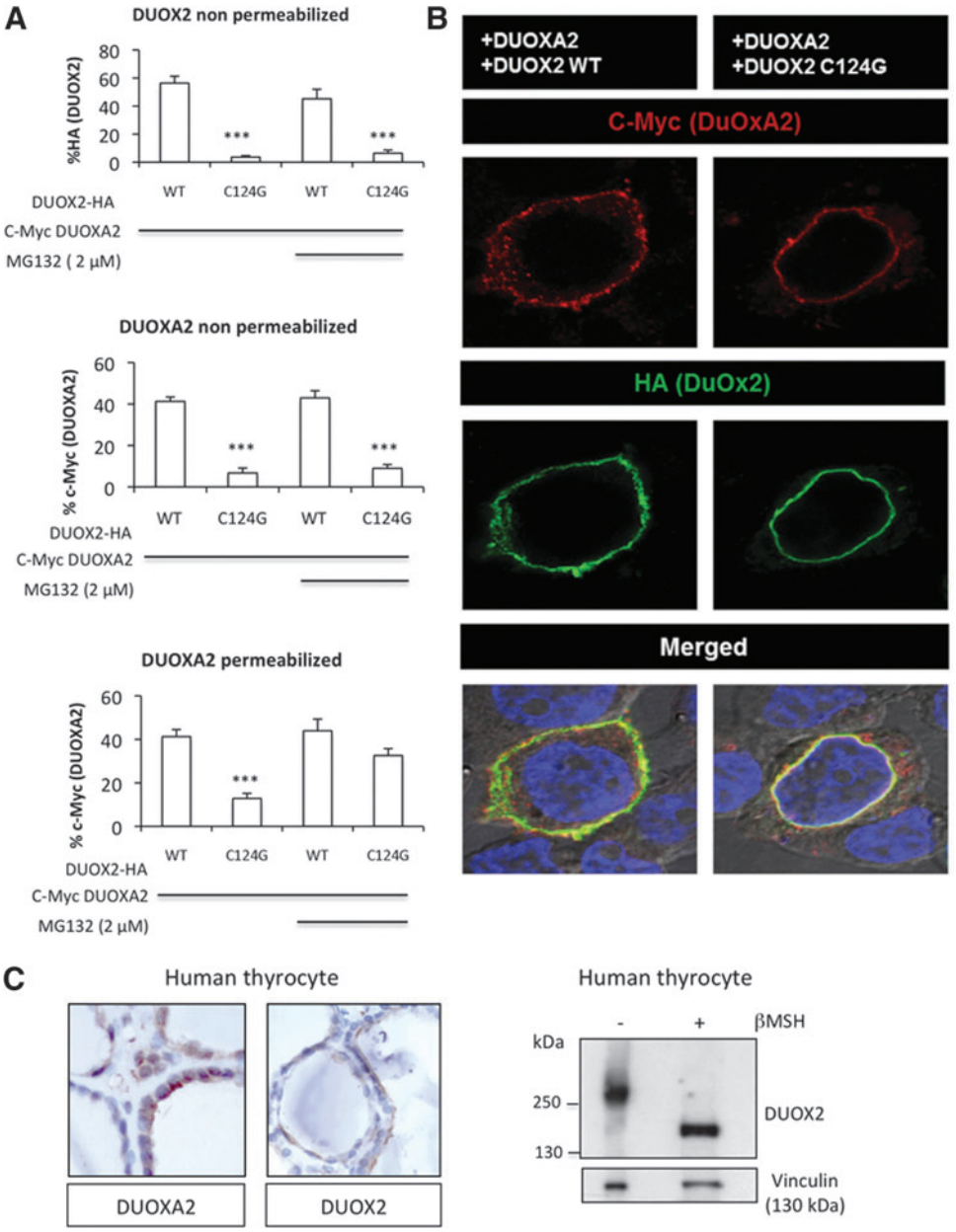


**FIG. 2. Defective plasma membrane targeting of mutant HA-DUOX2 C124G coexpressed with myc-DUOXA2.** **(A)** Representative histograms of flow immunocytofluorometry experiments. The *upper panel* shows that MG132 (2 $\mu M$) does not change the absence of expression of mutant HA-DUOX2 C124G at the cell surface. The *middle panel* shows that mutant HA-DUOX2 affects the cell surface targeting of myc-DUOXA2 in the presence or in the absence of MG132. The *bottom panel* shows that intracellular expression of myc-DUOXA2 in cells permeabilized with saponin is decreased in the presence of mutant HA-DUOX2, but MG132 rescues the inhibition. ***$P < 0.001$. **(B)** Surface expression of WT or mutant HA-DUOX2 C124G in permeabilized HEK293 cells cotransfected with myc-DUOXA2. Magnification ×63. The nuclei were stained with-DAPI. Note that mutant DUOX2 and its partner are condensed in a perinuclear zone **(C)** Localization of DUOX2 and DUOXA2 proteins at the apical surface of human thyrocytes analyzed by immunohistochemistry. Human thyrocytes were analyzed for DUOX2 expression under reducing and nonreducing conditions. HA, hemagglutinin.

WT DUOX2 was coexpressed in HEK293 cells with DUOXA2. Mutant DUOX2 C124G was taken as a control. To prevent proteasome-mediated DUOXA2 degradation, cells were treated with MG132 during the experiments. Cell lysates, prepared in nonreducing conditions, were then subjected to a proteomic analysis after immunoprecipitation with anti-DUOX2 antibody. Proteins were prefractionated by SDS-PAGE in nonreducing conditions (Fig. 3A). Proteomic analysis of bands with an apparent molecular mass superior to 150 kDa revealed that DUOXA2 only interacts with WT DUOX2 (Supplementary Fig. S1B). To check the interaction between DUOX2 and DUOXA2, C-terminal myc epitope-tagged DUOXA2 was coexpressed in HEK-293 cells with either WT DUOX2 or mutant DUOX2 C124G, and total proteins were analyzed under nonreducing conditions (Fig. 3B). Importantly, the c-Myc antibody immunodetected a band with an apparent molecular mass around 250 kDa where only WT DUOX2 was detected, indicating the existence of a disulfide bridge between DUOX2 and DUOXA2. To identify cysteine residues involved in the interaction between DUOX2 and DUOXA2, we performed immunoprecipitation experiments. C-terminal myc epitope-tagged DUOXA2 was coexpressed in HEK293 cells with each of the DUOX2 cysteine mutants. In the presence of MG132, DUOXA2 and each of all DUOX2 mutants were correctly expressed in cells, as shown in the analysis of input preparations (Fig. 3C). DUOXA2 coimmunoprecipitated with WT DUOX2 and mutants, DUOX2 C351G and C370G, found to be active at the cell surface. In contrast, there was no interaction with the other mutants of DUOX2, which are functionally inactive. Taken together, these data demonstrate for the first time that DUOXA2 interacts covalently with DUOX2 *via* disulfide bonds involving both cysteine residues 568 and 582 of DUOX2.

The acquisition of an intramolecular disulfide bond involving the cysteine 124 appeared to be the rate-limiting step in DUOX2 maturation. Therefore, we looked for cysteine residues present

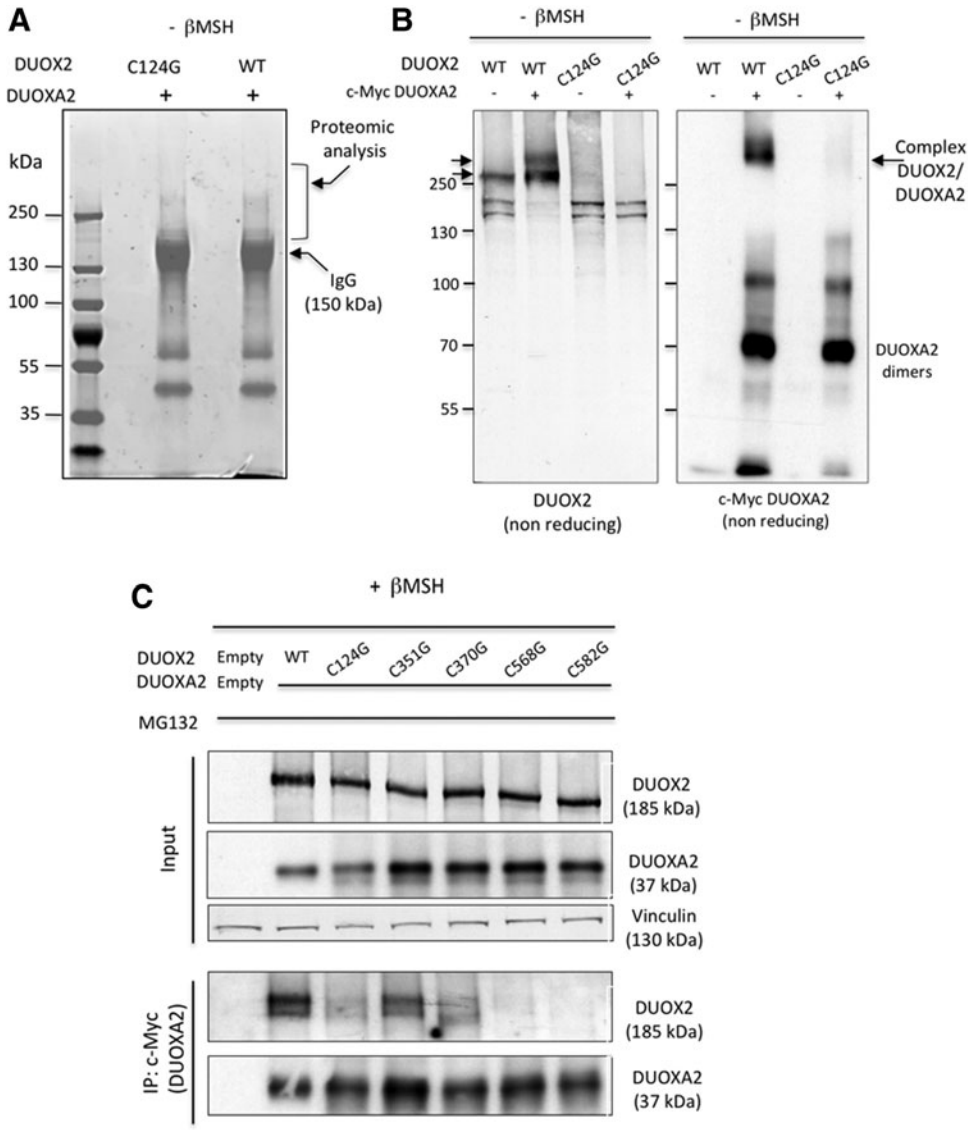


**FIG. 3. DUOXA2 interacts covalently with DUOX2. (A)** Immunoprecipitated DUOX2 and mutant DUOX2 C124G were analyzed by SDS-PAGE in nonreducing conditions. Proteins were stained as described under the Materials and Methods section. Bands with a molecular weight superior to 150 kDa were excised from the gel and microsequenced. **(B)** Covalent interaction between DUOX2 and DUOXA2 was analyzed by Western blot analysis in nonreducing conditions. DUOX2 or mutant DUOX2 C124G was coexpressed with myc-DUOXA2 in HEK293 cells. The expression of DUOX2 was detected by using anti-hDUOX2 and DUOXA2 was detected by using anti-myc. **(C)** Cells were cotransfected with DUOX2 or mutant DUOX2 and myc-DUOXA2. Anti-myc immunoprecipitates (IP: c-Myc) of the cell lysates were separated by SDS-PAGE in reducing conditions and analyzed by Western blotting for DUOX2 and myc-DUOXA2. Analysis of the cell lysates used as the input in immunoprecipitation is shown in the *upper three panels*. SDS-PAGE, sodium dodecyl sulfate–polyacrylamide gel electrophoresis.

in predicted extracellular loops of DUOX2 that could form a disulfide bridge with this cysteine residue located near the N-terminal extreme part of the ectodomain (Fig. 1A). Because cysteine residue 1162 appeared to be the only candidate, we evaluated, at first, the effect of its mutation on the $H_2O_2$-generating activity. This mutation not only suppressed the enzymatic activity but also the shift in the electrophoretic mobility of DUOX2 detected in nonreducing conditions, confirming that this cysteine is also involved in the oxidative folding of DUOX2 and forms an intramolecular disulfide bridge with cysteine 124. Consequently, mutation of cysteine 1162 also affected the stability of DUOXA2 (Fig. 4A) and the targeting at the plasma membrane of both DUOX2 and DUOXA2 (Fig. 4B). Importantly, immunoprecipitation experiments showed that mutation of cysteine 1162 prevented the covalent interaction between DUOX2 and its maturation factor (Fig. 4C).

### *How DUOXA2 interacts with DUOX2?*

Analysis of the human DUOXA1/2 sequence alignment shows that there are two conserved cysteines, cysteine 167 and cysteine 233, located within two different predicted extracellular domains that may form intermolecular disulfide bond(s) with DUOX2 (Fig. 5A). To explore the role of these cysteine residues, they were individually mutated to glycines. WT DUOX2 was coexpressed in HEK293 cells with either WT or each mutant, C167G and C233G, of DUOXA2. Treatment of cells with MG132 inhibited the degradation of either DUOXA2 mutant, indicating that C169G and C233G mutations generated unstable proteins (Supplementary Fig. S1C). These mutations affected the $H_2O_2$-generating activities by 50%, and treatment of cells with MG132 did not restore the activity (Fig. 5B). These data indicated that these cysteines are important for the function of the complex DUOX2/DUOXA2 and could be involved in a disulfide bridge with DUOX2. Analysis of protein expressions by Western blot in nonreducing conditions (Fig. 5C) and immunoprecipitation experiments (Fig. 5D) demonstrated that the cysteines, 167 and 233, of DUOXA2 are both involved in an intermolecular disulfide bridge with DUOX2.

## Discussion

In the present study, we have identified an intramolecular disulfide bridge between cys-124 and cys-1162 that is

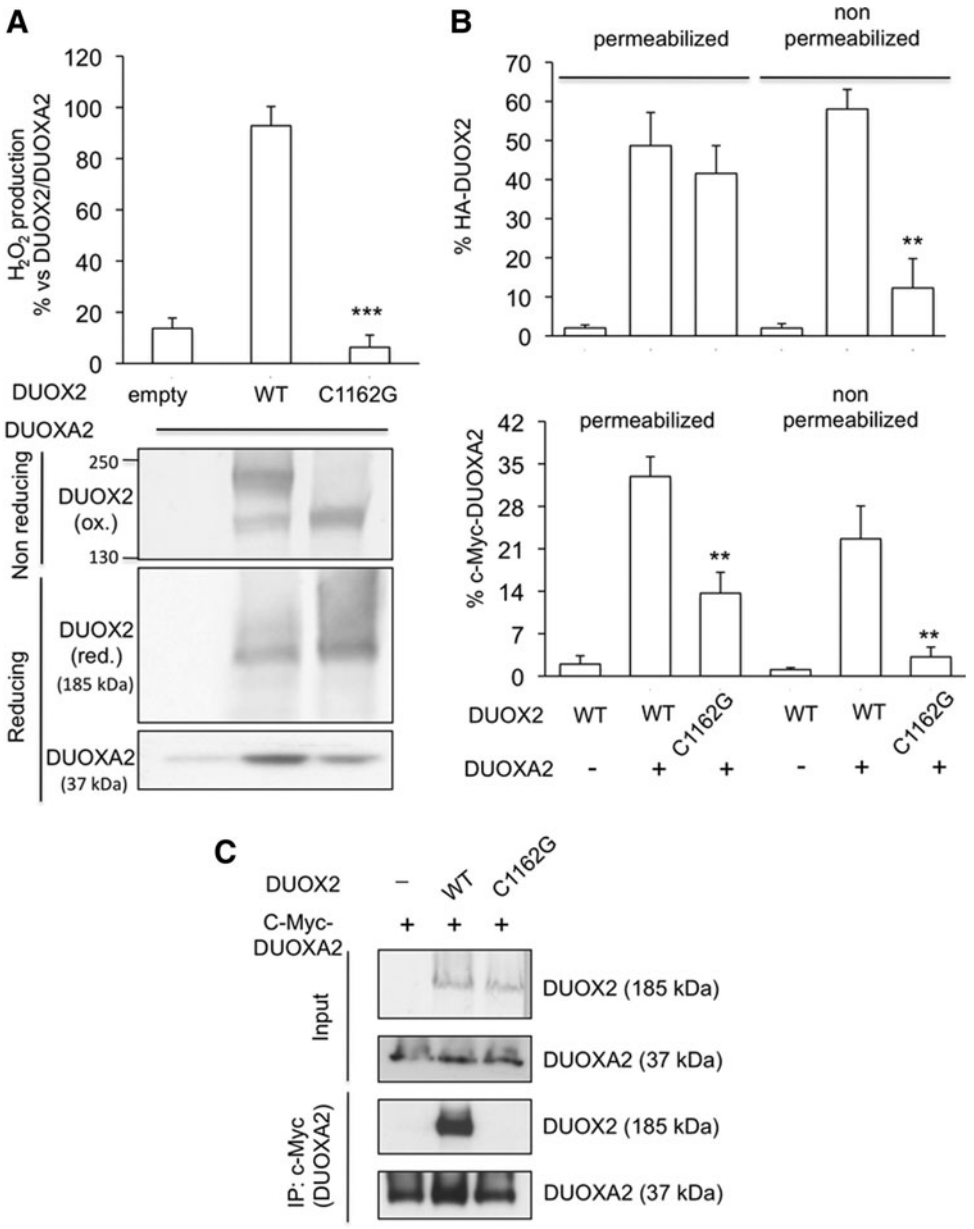


**FIG. 4. Cysteine 1162 is involved in the intramolecular disulfide bond essential for the activity and the targeting of DUOX2. (A)** HA-DUOX2 (WT) and mutant HA-DUOX2 C1162G proteins were transiently expressed with DUOXA2 protein in HEK293 cells. The extracellular $H_2O_2$-generating activity was measured after 48 h. The expression of the WT and mutant DUOX2 was analyzed by immunoblotting in nonreducing and reducing conditions. DUOXA2 expression was assessed by using anti-DUOXA2 antibody. ***$P < 0.001$. **(B)** Representative histograms of flow immunocytofluorometry experiments. Absence of cell surface expression of the mutant HA-DUOX2 C1162G was associated with an absence of cell surface expression of N-terminal cMyc epitope-tagged human DUOXA2. **$P < 0.01$. **(C)** Cells were cotransfected with HA-DUOX2 or mutant HA-DUOX2 C1162G in the presence of myc-DUOXA2. Anti-myc immunoprecipitates of the cell lysates were separated by SDS-PAGE and analyzed by Western blotting. Analysis of the cell lysates used as the input in immunoprecipitation is shown in the *upper two panels.*

essential for the structure and the function of DUOX2. These two cysteine residues reside, respectively, in the N-terminal ectodomain and in an extracellular loop connecting TMs 4 and 5 of the DUOX. Therefore, these cysteines, which are distant in the linear sequence, appear to be in close proximity in the native protein. At first sight, this was unexpected because, most of the time, intramolecular disulfide bonds form between adjacent cysteines located in the same loop. Thus, in this context, it was rather considered initially that cys-124 forms, in the first place, a disulfide bridge with one of the four other cysteine residues located in the N-terminal ectodomain since they enter the ER lumen first. Once again, this finding highlights the complexity of the process related to the protein folding in the ER.

The existence of this intramolecular bridge, which appears to have some functional significance, has been evidenced by a shift in the electrophoretic mobility for the WT DUOX2 under nonreducing conditions that is eliminated by mutation of either cysteine 124 or cysteine 1162. Of importance, this shift is not restricted to the recombinant expression system used for this study. It was also observed in human primary thyrocytes where DUOX2 is well expressed, indicating that the oxidative folding of DUOX2 takes place in physiological conditions. We cannot exclude that other cysteines in the DUOX2 can form intramolecular disulfide bonds, but our results demonstrate the importance of both cysteine 124 and cysteine 1162 in a conformation-dependent mobility shift.

The structure of the N-terminal ectodomain of DUOX2 by itself promotes the formation of the intramolecular bridge between the cysteine residues, 124 and 1162. Thus, any mutation in the N-terminal domain that modifies its own conformation may prevent the formation of this intramolecular disulfide bond. This was probably the case for two natural DUOX2 mutants (Q36H and R376W) implicated in congenital hypothyroidism for which the absence of

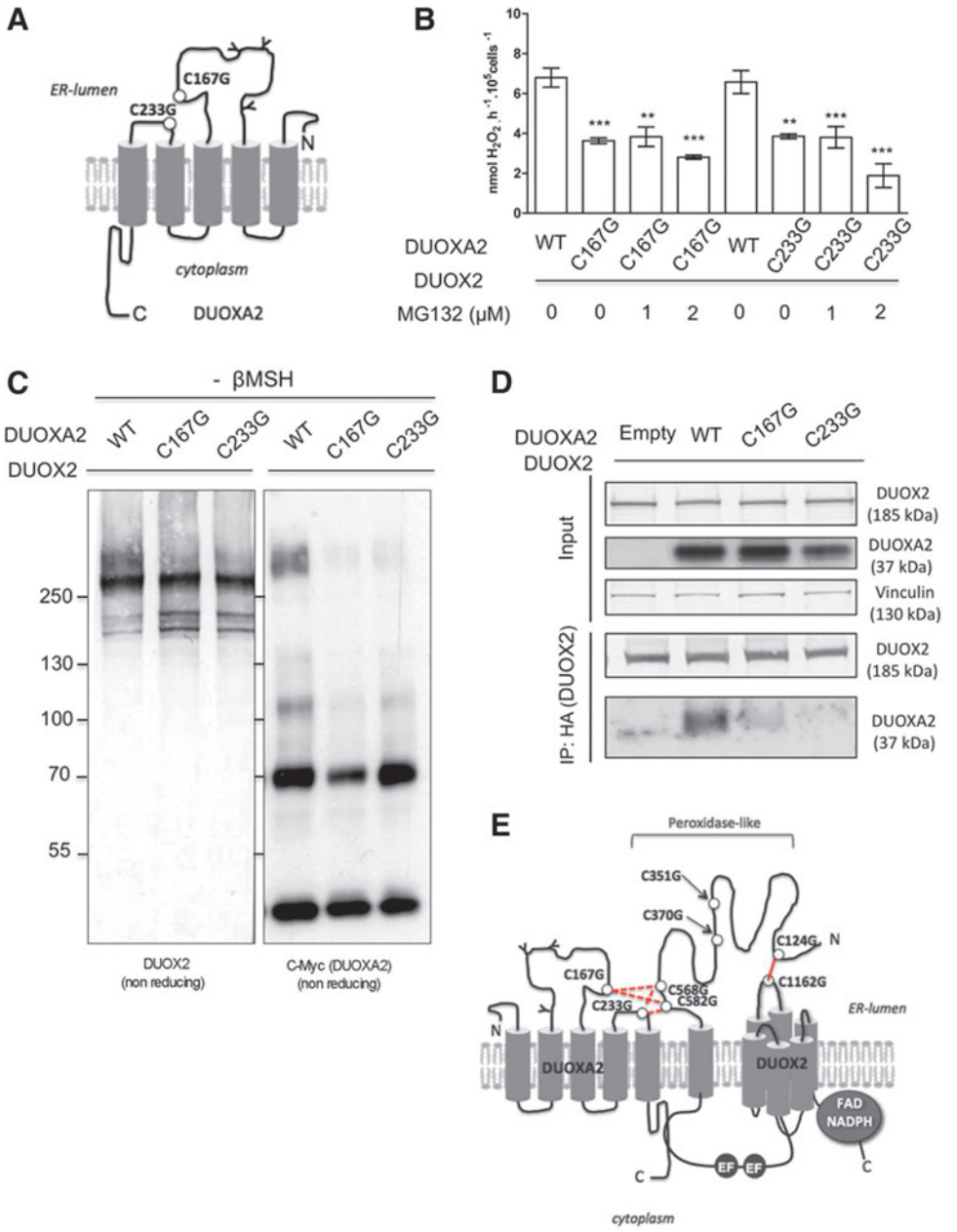


**FIG. 5. Cysteines, 167 and 233, of DUOXA2 form disulfide bonds with DUOX2.** **(A)** Schematic representation of DUOXA2 with the proposed topology in the membrane. The *circles* indicate the relative positions of mutated cysteine residues. **(B)** C-terminal cMyc epitope-tagged DUOXA2 (WT) and C-terminal cMyc epitope-tagged mutant DUOXA2 C167G or C233G proteins were transiently expressed with WT DUOX2 protein in HEK293 cells treated with increasing concentrations of MG132. $^{**}P < 0.01$, $^{***}P < 0.001$. **(C)** Expression of DUOX2 and DUOXA2 proteins analyzed by immunoblotting in nonreducing conditions by using, respectively, anti-DUOX2 and anti-myc antibodies. **(D)** Cells were cotransfected with HA-DUOX2 in the presence of WT DUOXA2-myc or mutant DUOXA2-myc. Anti-HA immunoprecipitates of the cell lysates were separated by SDS-PAGE in reducing conditions and analyzed by Western blotting by using anti-DUOX2 and anti-myc, respectively. Analysis of the cell lysates used as input in immunoprecipitation is shown in the *upper two panels*. **(E)** Schematic representation of the DUOX2/DUOXA2 complex in the cell membrane. The intramolecular bond between DUOX2 cysteine residues 124 and 1162 is indicated. The intermolecular bonds between DUOX2 and DUOXA2 involved, respectively, N-terminal cysteine residues 568 and 582 of DUOX2 and cysteine residues 167 and 233 of DUOXA2. Several combinations are considered.

trafficking and activity was related to the absence of the oxidized form (10).

In general, intramolecular disulfide bridge formation is critically important for the stability of the neosynthesized protein and determines its own fate, that is, degradation or targeting to the plasma membrane. Importantly, the oxidative folding of DUOX2 was found to also determine the fate of its maturation factor, DUOXA2. Suppression of the intramolecular disulfide bond in DUOX2 induced preferentially a degradation of DUOXA2, highlighting that the oxidized form of DUOX2 influences the stability of its own partner. However, the inhibition of proteasomal protein degradation of

DUOXA2 by MG132 was not sufficient to restore the targeting to the plasma membrane and therefore the $H_2O_2$-generating activity of the DUOX. The function of DUOXA2 was also altered, indicating that it is totally dependent on a well-defined conformation of the N-terminal ectodomain of DUOX2. Recently, except for cysteine 124, the four cysteine residues ($Cys^{351}$, $cys^{370}$, $Cys^{568}$, and $Cys^{582}$) were mapped onto a structural model of an isolated DUOX2 N-terminal region (13). Each cysteine residue was found to exist as a solvent-exposed residue situated on one face of the protein surface, suggesting that it may enable protein–protein interaction that is required for maturation. Mutations of two of these cysteines, that is, cys-568 and cys-582, that did not prevent the oxidative folding of DUOX2, were found to impair both stability and function of DUOXA2 (Fig. 1B). Our findings show that these two cysteines are involved in covalent interactions through disulfide bridges with cysteines, 167 and 233, located in two different extracellular loops of the maturation factor, DUOXA2. These intermolecular disulfide bonds, important for the stability of DUOXA2, play therefore a critical role in both targeting and functioning of the DUOX at the plasma membrane.

In conclusion, we have identified an intramolecular disulfide bridge that is essential for the structure and the function of DUOX2. This disulfide bridge formed in the ER appears to be a key event in the trafficking of the DUOX2/DUOXA2 complex as it promotes an appropriate conformation of the N-terminal region, which is propitious to subsequent covalent interactions through disulfide bridges with the maturation factor, DUOXA2 (Fig. 5E). We highlighted that both stability and function of DUOXA2 are totally dependent on the oxidative folding of DUOX2. These findings change the paradigm concerning the nature of the relationship between the two proteins and provide us with opportunities to design potential therapeutics targeting this DUOX2-DUOXA2 interaction to control the DUOX2-dependent $H_2O_2$-generating activity that could be deleterious in pathological conditions.

## Materials and Methods

### *Cell culture, mutagenesis, and transfection*

HEK293 cells were cultured in DMEM (high glucose; PAA) supplemented with 10% (v/v) fetal calf serum and penicillin/streptomycin (100 $\mu$g/ml; Life Technologies Ltd). Primary human thyroid cells were cultured as previously described (19). Normal, human thyroid tissue specimens were collected at Institut Gustave Roussy in accordance with local and national ethics laws. Informed consent was obtained from all patients.

The mutagenesis of cysteine residues has been previously performed by using the QuikChange site-directed mutagenesis kit (Stratagene) and a pcDNA3 plasmid containing the full-length human (h) WT DUOX2 (hDUOX2-pcDNA3) as a template (7). The NH2-terminal hemagglutinin epitope-tagged human DUOX2 (HA-DUOX2-pcDNA3), kindly given by Dr. Xavier de Deken (Brussels, Belgium), and the NH2-terminal cMyc epitope-tagged human DUOXA2 as the COOH-terminal cMyc epitope-tagged human DUOXA2 (cMyc-DUOXA2-pcDNA3) were described elsewhere (9).

In transient cell transfection experiments, HEK293 cells reaching 50%–70% confluence were transfected in 24-well plates using X-tremeGENE HP DNA Transfection Reagent with the protocol recommended by the manufacturer (Roche). At 24 h after transfection, the medium was changed and 20 $\mu M$ hemin was added, and the transfected cells were treated with the test agents for the times and at the concentrations indicated in each experiment. After 48 h, the cells were harvested.

### *Measurement of $H_2O_2$ generation*

$H_2O_2$ generation was quantified by the Amplex red/horseradish peroxidase assay (Sigma Aldrich), which detects the accumulation of a fluorescent oxidized product. Cells ($2\times10^4$) in Dulbecco's phosphate-buffered saline (D-PBS) with $CaCl_2$ and $MgCl_2$ were incubated with D-glucose (1 mg/ml), ionomycin (1 $\mu M$; Sigma Aldrich), SOD (100 U/ml; Sigma Aldrich), horseradish peroxidase (0.5 U/ml; Roche), and Amplex red (50 $\mu M$; Sigma Aldrich), and immediately the fluorescence was measured in a microplate reader (Victor3; PerkinElmer) at 37°C for 30 min using excitation at 530 nm and emission at 595 nm. Particulate fractions (75 $\mu$g) were incubated in 50 m$M$ sodium phosphate buffer (pH 7.2) containing sucrose (150 m$M$), EGTA (1 m$M$), $CaCl_2$ (1.5 m$M$), SOD (200 U/ml), horseradish peroxidase (0.5 U/ml), and Amplex red (50 $\mu M$). The reaction was started by adding 0.1 m$M$ NADPH and the fluorescence was measured as described above. $H_2O_2$ release was quantified (nanomoles $H_2O_2$ per hour per $10^5$ cells) using standard calibration curves.

### *Preparation of the cellular particulate fraction*

Cells were washed with PBS and scraped into the same solution supplemented with a mixture of protease inhibitors (5 $\mu$g/ml aprotinin, 5 $\mu$g/ml leupeptin, 1 $\mu$g/ml pepstatin, 157 $\mu$g/ml benzamidine). After centrifuging at 200 $g$ for 10 min at 4°C, the cell pellet was homogenized using a motor-driven Teflon pestle homogenizer in 2 ml of 50 m$M$ sodium phosphate buffer containing 0.25 M sucrose, 0.1 m$M$ dithiothreitol, 1 m$M$ EGTA (pH 7.2), and the mixture of protease inhibitors. After centrifuging at 200,000 $g$ for 30 min, the pellet was resuspended in 0.5 ml of 50 m$M$ sodium phosphate buffer (pH 7.2) containing 0.25 M sucrose, 1 m$M$ $MgCl_2$, and the mixture of protease inhibitors.

### *Western blot analysis*

Cell extracts were prepared as previously described (19) by adding 20 m$M$ NEM in lysis buffer. Samples were then sonicated for 15 s. Protein samples (10–30 $\mu$g) supplemented with or without 2.5% (v/v) ß-mercaptoethanol and 10% glycerol were denatured for 2 min at 100°C, subjected to SDS-PAGE using a 4%–12% or 8%–16% tris-glycine polyacrylamide minigel (Life Technologies Ltd), and electrotransferred to 0.2-$\mu$m Protran BA83 nitrocellulose sheets (Schleicher & Schuell). The immunodetection of DUOX2 was done as previously described (14). Anti-DUOXA2 has been previously described (20). Immunodetection was also done by using primary antibodies: anti-vinculin (Abcam), anti-HA (clone 3F10; Roche), and anti-cMyc (Santa Cruz Biotechnology).

### *Immunoprecipitation*

After preparation of particulate fractions, protein pellets were incubated overnight with Nonidet P40 at 4°C in nonreducing conditions. After centrifugation, soluble proteins were immunoprecipitated (IP) with Myc or HA antibody as recommended by the kit manufacturer (Sigma Aldrich).

### *Proteomic study*

HEK293 cells were transiently cotransfected with WT DUOX2 or mutant DUOX2 in the presence of DUOXA2. Twelve hours before harvesting, the cells were treated with 1 $\mu M$ of MG132. The cells from two Petri dishes (about $2 \times 10^7$ cells) were then lysed in 0.5 ml 10 m$M$ Tris/HCl buffer, pH 7.5, containing 150 m$M$ NaCl, 0.5% Nonidet P40, 2 m$M$ EDTA, 20 m$M$ NEM, and a cocktail of protease inhibitors (SIGMA). The lysate was incubated overnight at 4°C and centrifuged at 200,000 $g$ for 30 min. The supernatant was used for immunoprecipitation experiments. DUOX2 and mutant DUOX2 were IP in nonreducing conditions by using the Dynabeads Protein A immunoprecipitation kit (Invitrogen) with an antibody raised against the first intracellular domain $Glu^{636}$-$Arg^{1039}$ of human DUOX2 *(anti-hDUOX2)*. The Ab-Ag complex was eluted with the nonreducing SDS-PAGE sample buffer before being subjected to migration using a 4%–12% linear gradient polyacrylamide slab minigel (Invitrogen). Proteins were stained by using the colloidal blue staining kit (Invitrogen), and bands were excised from gels.

### *In gel digestion*

The gel bands were washed first with 100 $\mu$l of ammonium bicarbonate 25 m$M$ (SIGMA 11204)/acetonitrile (SIGMA 34967) 50/50 v/v by mixing for 10 min at room temperature (RT), then with 100 $\mu$l of 100% acetonitrile by mixing for 10 min at RT. These two steps were repeated once in the same order. Samples were dried on a speed vac for 2 min. Twenty microliters of trypsin (Calbiochem 650279) at 11.55 ng/$\mu$l was added to each gel piece. After incubation at RT for 15 min, 20 $\mu$l of ammonium bicarbonate 50 m$M$ was added. Samples were incubated at 37°C overnight. Supernatants were separated from gel pieces and transferred to analysis vials. Twenty microliters of formic acid 5% (SIGMA 33015-1l)/acetonitrile 30/70 v/v was added to each piece of gel to extract remaining peptides. Supernatants were combined together and then dried on the speed vac. Ten microliters of 97% water, 3% acetonitrile, and 0.1% formic acid was added to solubilize the tryptic peptides.

### *Analysis on nanoHPLC-chip cube ion trap (Agilent)*

The tryptic peptide mixtures were analyzed with nanoHPLC (Agilent Technologies 1200) directly coupled to an ion trap mass spectrometer (BRUKER 6300 series) equipped with a nanoelectrospray source. Three microliters of the peptide mixture was separated on ProtID-Chip-43 II 300A C18 43 mm col (G4240-62005 Agilent) with a 30 min-gradient from 3% to 97% of acetonitrile.

The acquisition was performed as following: one full-scan MS over the range of 200–2200 m/z, followed by three data-dependent MS/MS scans on the three most abundant ions in the full scan. The data were analyzed on the Spectrum Mill MS Proteomics Workbench Rev A.03.03.084 SR4 with the following settings: DATA EXTRACTOR: MH + 200–4400 Da; Scan range 0–30 min.

MS/MS SEARCH: Swiss-Prot database; Homo sapiens; trypsin; two missed cleavages; oxidized methionine (M), phosphorylated S, T, Y: masses are monoisotopic; and precursor mass tolerance ± 2 Da and product mass tolerance ± 0.8 Da.

### *Flow immunocytofluorometry*

For surface protein staining, cells were detached from the plates with PBS containing 5 m$M$ EDTA/EGTA and incubated for 30 min at RT with a rat anti-HA of high affinity (clone 3F10; Roche) or with a mouse monoclonal anti-Myc (Santa Cruz Biotechnology), respectively, for NH2-terminal HA epitope-tagged human DUOX2 and NH2-terminal cMyc epitope-tagged human DUOXA2 surface immunofluorescence staining. The samples were washed once with D-PBS/0.1% bovine serum albumin (BSA) and incubated for 30 min with Alexa 488-conjugated antirat IgG or Alexa 568-conjugated antimouse IgG diluted in D-PBS/0.1% BSA (Life Technologies Ltd). After two washing steps, the cells were resuspended in D-PBS/0.1% BSA. For detection of intracellular HA-DUOX2 or DUOXA2-myc, detached cells were fixed in 1% paraformaldehyde/D-PBS for 10 min at 4°C, washed in D-PBS, and permeabilized for 20 min with 0.2% saponin in D-PBS/0.1% BSA. Binding of antibodies was done as above. Fluorescence was assayed using a BD Accuri™ C6 Flow Cytometer (BD Biosciences), counting 10,000 events per sample. Relative protein expression was determined by calculating differences in total fluorescence between the sample and an equal-sized population of pcDNA3-DUOX2 and pcDNA3-DUOXA2-transfected cells corresponding to 100%.

### *Immunofluorescence studies*

Transfected cells grown on glass coverslips were washed in D-PBS and fixed in 4% paraformaldehyde/D-PBS for 10 min. Nonspecific binding sites were blocked with 3% BSA/D-PBS for 30 min. For staining of NH2-terminal HA epitope-tagged human DUOX2 or NH2-terminal cMyc epitope-tagged human DUOXA2, cells were incubated for 2 h with rat anti-HA clone 3F10 or with mouse anti-Myc in TBS buffer containing 0.3% BSA. After three washing steps in TBS with 0.1% Tween, Alexa 488-conjugated anti-rat IgG or Alexa 568-conjugated anti-mouse IgG diluted in TBS/0.3% BSA (Life Technologies Ltd) was used as the secondary antibody. After two washing steps in TBS 0.1% Tween and staining with Hoechst 33342 fluorochrome (Life Technologies Ltd), the slides were mounted with Dako Fluorescence Mounting Medium (Dako Denmark). Fluorescent images were captured on a confocal microscope (Leica DM IRE 2; Perkin Elmer).

### *Statistical analysis*

Data are represented as the means ± standard deviations of the results of at least three independent experiments. Student's $t$-test was used to calculate significance values. Significant values are indicated as (*) $p$-value of $< 0.05$ or (**) $p$-value of $< 0.01$ or (***) $p$-value of $< 0.001$.

## Acknowledgments

The authors are indebted to Monique Talbot for her excellent assistance in immunohistochemistry and Emilie Cochet for her excellent assistance in proteomic. A.C. was supported by the Institut National du Cancer (INCa, France), and R.A.N.L. was supported by CAPES-COFECUB. S.M. and T.L.L were supported by funds from the Intramural Research Program of the National Institute of Allergy and Infectious Diseases, NIH. This work was supported by a grant from INCA.

### Author Disclosure Statement

No competing financial interests exist.

### References


1. Aerssens J, Camilleri M, Talloen W, Thielemans L, Göhlmann HW, Van Den Wyngaert I, Thielemans T, De Hoogt R, Andrews CN, Bharucha AE, Carlson PJ, Busciglio I, Burton DD, Smyrk T, Urrutia R, and Coulie B. Alterations in mucosal immunity identified in the colon of patients with irritable bowel syndrome. *Clin Gastroenterol Hepatol* 6: 194–205, 2008.
2. Csillag C, Nielsen OH, Vainer B, Olsen J, Dieckgraefe BK, Hendel J, Vind I, Dupuy C, Nielsen FC, and Borup R. Expression of the genes dual oxidase 2, lipocalin 2 and regenerating islet-derived 1 alpha in Crohn's disease. *Scand J Gastroenterol* 42: 454–463, 2007.
3. De Deken X, Wang D, Dumont JE, and Miot F. Characterization of ThOX proteins as components of the thyroid H(2)O(2)-generating system. *Exp Cell Res* 273: 187–196, 2002.
4. De Deken X, Wang D, Many MC, Costagliola S, Libert F, Vassart G, Dumont JE, and Miot F. Cloning of two human thyroid cDNAs encoding new members of the NADPH oxidase family. *J Biol Chem* 275: 23227–23233, 2000.
5. Dupuy C, Ohayon R, Valent A, Noel-Hudson MS, Deme D, and Virion A. Purification of a novel flavoprotein involved in the thyroid NADPH oxidase. Cloning of the porcine and human cdnas. *J Biol Chem* 274: 37265–37269, 1999.
6. Ellgaard L and Helenius A. Quality control in the endoplasmic reticulum. *Nat Rev Mol Cell Biol* 4: 181–191, 2003.
7. Fortunato RS, Lima de Souza EC, Ameziane-el Hassani R, Boufraqech M, Weyemi U, Talbot M, Lagente-Chevallier O, de Carvalho DP, Bidart JM, Schlumberger M, and Dupuy C. Functional consequences of dual oxidase-thyroperoxidase interaction at the plasma membrane. *J Clin Endocrinol Metab* 95: 5403–5411, 2010.
8. Geiszt M, Witta J, Baffi J, Lekstrom K, and Leto TL. Dual oxidases represent novel hydrogen peroxide sources supporting mucosal surface host defense. *FASEB J* 17: 1502–1504, 2003.
9. Grasberger H and Refetoff S. Identification of the maturation factor for dual oxidase. Evolution of an eukaryotic operon equivalent. *J Biol Chem* 281: 18269–18272, 2006.
10. Grasberger H, De Deken X, Miot F, Pohlenz J, and Refetoff S. Missense mutations of dual oxidase 2 (DUOX2) implicated in congenital hypothyroidism have impaired trafficking in cells reconstituted with DUOX2 maturation factor. *Mol Endocrinol* 21: 1408–1421, 2007.
11. Hornsby MJ, Huff JL, Kays RJ, Canfield DR, Bevins CL, and Solnick JV. Helicobacter pylori induces an antimicrobial response in rhesus macaques in a cag pathogenicity island-dependent manner. *Gastroenterology* 134: 1049–1057, 2008.
12. Luxen S, Noack D, Frausto M, Davanture S, Torbett BE, and Knaus UG. Heterodimerization controls localization of Duox-DuoxA NADPH oxidases in airway cells. *J Cell Sci* 122: 1238–1247, 2009.
13. Meitzler JL, Hinde S, Bánfi B, Nauseef WM, and Ortiz de Montellano PR. Conserved cysteine residues provide a protein-protein interaction surface in dual oxidase (DUOX) proteins. *J Biol Chem* 288: 7147–7157, 2013.
14. Morand S, Agnandji D, Noel-Hudson MS, Nicolas V, Buisson S, Macon-Lemaitre L, Gnidehou S, Kaniewski J, Ohayon R, Virion A, and Dupuy C. Targeting of the dual oxidase 2 N-terminal region to the plasma membrane. *J Biol Chem* 279: 30244–30251, 2004.
15. Morand S, Ueyama T, Tsujibe S, Saito N, Korzeniowska A, and Leto TL. DUOX maturation factors form cell surface complexes with DUOX affecting the specificity of reactive oxygen species generation. *FASEB J* 23: 1205–1218, 2009.
16. Moreno JC, Bikker H, Kempers MJ, van Trotsenburg AS, Baas F, de Vijlder JJ, Vulsma T, and Ris-Stalpers C. Inactivating mutations in the gene for thyroid oxidase 2 (THOX2) and congenital hypothyroidism. *N Engl J Med* 347: 95–102, 2002.
17. Varela V, Rivolta CM, Esperante SA, Gruneiro-Papendieck L, Chiesa A, and Targovnik HM. Three mutations (p.Q36H, p.G418fsX482, and g.IVS19-2A>C) in the dual oxidase 2 gene responsible for congenital goiter and iodide organification defect. *Clin Chem* 52: 182–191, 2006.
18. Vigone MC, Fugazzola L, Zamproni I, Passoni A, Di Candia S, Chiumello G, Persani L, and Weber G. Persistent mild hypothyroidism associated with novel sequence variants of the DUOX2 gene in two siblings. *Hum Mutat* 26: 395–403, 2005.
19. Weyemi U, Caillou B, Talbot M, Ameziane-El-Hassani R, Lacroix L, Lagent-Chevallier O, Al Ghuzlan A, Roos D, Bidart JM, Virion A, Schlumberger M, and Dupuy C. Intracellular expression of reactive oxygen species-generating NADPH oxidase NOX4 in normal and cancer thyroid tissues. *Endocr Relat Cancer* 17: 27–37, 2010.
20. Zamproni I, Grasberger H, Cortinovis F, Vigone MC, Chiumello G, Mora S, Onigata K, Fugazzola L, Refetoff S, Persani L and Weber G. Biallelic inactivation of the dual oxidase maturation factor 2 (DUOXA2) gene as a novel cause of congenital hypothyroidism. *J Clin Endocrinol Metab* 93: 605–610, 2008.



Address correspondence to:
*Dr. Corinne Dupuy*
*Institut Gustave Roussy*
*UMR 8200 CNRS*
*114 rue Edouard Vaillant*
*94805 Villejuif cedex*
*France*

*E-mail:* corinne.dupuy@gustaveroussy.fr


Date of first submission to ARS Central, January 22, 2015; date of final revised submission, February 27, 2015; date of acceptance, March 11, 2015.

**Abbreviations Used**

BSA = bovine serum albumin
DUOX = dual oxidase
DUOXA = DUOX activator
ER = endoplasmic reticulum
HA = hemagglutinin
IP = immunoprecipitated;
NADPH = reduced nicotinamide adenine dinucleotide phosphate
NEM = N-ethylmaleimide
NOX = NADPH oxidase
SDS-PAGE = sodium dodecyl sulfate–polyacrylamide gel electrophoresis
WT = wild-type